Arch. Metall. Mater. **62** (2017), 4, 2051-2056

DOI: 10.1515/amm-2017-0304

P. SOCHACKA*#, A. MIKLASZEWSKI*, M. JURCZYK*

THE INFLUENCE OF Mo CONTENT ON PHASE TRANSFORMATION IN Ti-Mo ALLOYS

Titanium β-type alloys are a class of interesting biomaterials that can exhibit a unique combination of mechanical as well as physicochemical and biological properties. The aim of this study is to develop a titanium-molybdenum alloys (Ti-x at % Mo, x = 15 and 23). These materials were prepared by the combination of mechanical alloying and powder metallurgical process. The details of the processing method were presented. The samples were characterized by X-ray diffraction, scanning electron microscopy, chemical composition determination as well as density and Vickers microhardness measurements. The corrosion behaviour in Ringer solution was investigated, too. The crystallization of the obtained material upon annealing led to the formation of a near single β type alloys. The molybdenum content in titanium and heat treatment parameters of a nearly amorphous phase allow to synthesize Ti(β)-type alloys. The present study has demonstrated that Ti23Mo alloy can be the next generation of biomaterial for bone tissue engineering.

Keywords: Titanium, Molybdenum, Biomaterials, Mechanical alloying, Phase transitions α-β

1. Introduction

Titanium and titanium alloys are preferred materials in the production of implants. Current research focuses on improving the mechanical performance and biocompatibility of Ti-based systems through variations in alloy composition, microstructure and surface treatment [1,2]. In the case of titanium, significant efforts go into enhancing the strength characteristics of commercial purity grades in order to avoid potential biotoxicity of alloying elements, especially in medical implants. To enhance the physicochemical and mechanical performance of implant materials through microstructure control, the top-down approaches known as severe plastic deformation (SPD) [3] and mechanical alloying (MA) [4] techniques were applied.

Mechanical alloying, the main mechanical process, was developed in the 1970s [4]. During the last years, the MA process has been successfully used to prepare a variety of alloy powders including powders exhibiting supersaturated solid solutions, amorphous phases, and nano-intermetallic compounds. The raw materials used for MA, are available commercially high purity powders with the sizes in the range of 1-100 μm. During the mechanical alloying process, the powder particles are periodically trapped between colliding balls and are plastically deformed. Such a feature occurs by the generation of a wide number of dislocations as well as other lattice defects. Furthermore, the ball collisions cause fracturing and cold welding of the elementary particles, forming clean interfaces at the atomic scale. Further milling lead to an increase of the interface number and the sizes of the elementary component area decrease from millimeter to submicrometer lengths. Concurrently to this decrease of the elementary distribution, some nanocrystalline intermediate phases are produced inside the particles or at its surfaces. As the milling duration develops, the content fraction of such intermediate compounds increases leading to a final product whose properties are the function of the milling conditions.

Recent studies showed clearly that nanostructuring of titanium can considerably improve not only the mechanical properties but also the biocompatibility [5,6]. For example, the strength of the nanostructured titanium is nearly twice of that of conventional cp titanium. Additionally, it has been shown, that the fatigue strength of nanostructured cp titanium at 10^6 cycles is almost two times higher than for conventional cp titanium and exceeds that of the Ti-6Al-4V alloy [7].The past few years, application of nanoscale biomaterials has become very popular in medicine [8].

While these biomaterials have been successful at encouraging bone ingrowth both *in vivo* and in clinical trials, the range of materials and microstructures available is still rather limited. To optimize Ti-based alloys for medical implant applications, several studies has focused on the design of biomaterials with optimized architecture to fulfil physicochemical, mechanical as well as regeneration requirements. The goals in the development of new Ti-based biomaterials are: (i) to avoid potentially toxic elements, such as vanadium, to further improve biocompatibility; (ii) to produce titanium alloys with a high fatigue strength. Currently, it is possible to prepare β-type titanium alloys with

* POZNAN UNIVERSITY OF TECHNOLOGY, INSTITUTE OF MATERIALS SCIENCE AND ENGINEERING, 5 MARII SKŁODOWSKIEJ-CURIE SQ., 60-965, POZNAN, POLAND

Corresponding author: patrycja.sochacka@doctorate.put.poznan.pl

excellent biocompatibility [9,10]. For example, Ti-6Al-7Nb [11], Ti-40Zr [12] and Ti-Mo-X (X = Al, Ga, Ge) [13] are attractive for medical applications.

The aim of this work was synthesis of titanium-molybdenum (Ti-x at. % Mo, x = 15 and 23) alloys by mechanical alloying and powder metallurgy methods and their characterization. The influence of Mo content and heat treatment temperature on phase transitions (Ti(α)-Ti(β)) were studied.

2. Materials and methods

Commercial powders of titanium (<45 μm, 99.9%, Alfa Aesar) and molybdenum (44 μm, 99.6%, Sigma Aldrich) were used. Mechanical alloying at argon atmosphere was performed using SPEX 8000 Mixer Mill for 48 h. Elemental powders Ti and Mo were weighted, blended and poured into vials in glove box (Labmaster 130) filled with automatically controlled argon atmosphere (O_2 < 2 ppm and H_2O < 1 ppm). A weight ratio of hard steel balls (10 mm diameter) to powder weight ratio equalled 10:1. In the next step, the produced powders were placed into the matrix and uniaxially pressed at a pressure of 600 MPa. Finally, the green compacts were heated through 1 h to 750, 800 or 850°C, and kept at high temperature for 30 min for sintering. After that, the sinters were slowly cooled down to room temperature together with the furnace. The diameter and height of bulk samples were 8 mm and 4 mm, respectively.

The crystallographic structure of the samples during different processing stages was investigated at room temperature by XRD method using a Panalytical Empyrean equipment with the CuKα (λ = 1.54056 Å) radiation. Measurements were carried out over an angular range of 30-60° with a scanning step of 0.02 and counting time of 30 s. Obtained spectra were refined for parameters and variables as a background and profile coefficients, lattice parameters, linear absorption coefficients. The instrumental broadening effect for collected data was eliminated by subtracting the full width at half-maximum (β_o) of a standard (Si) sample from β of the respective Bragg peaks. The Williamson-Hall (W-H) analysis method was used to study crystallite size and lattice strain on the peak broaden of the obtained mechanical alloyed powders spectra. Each point at linear W-H analysis is assigned to a specific diffraction line, after the point collection, a linear regression should give a linear fit which allows to estimate the material strain component from the slope and the size component from the intercept. Scanning electron microscope (SEM, VEGA 5135 Tescan) with energy dispersive spectrometer (EDS) was used to characterize the chemical composition of the prepared samples.

The porosity of the porous materials was calculated by the formula $P = (1 - \rho/\rho_{th}) \times 100\%$, where ρ and ρ_{th} are the density of the porous material and its corresponding theoretical density calculated for the rule of the mixtures, respectively. The density of the sintered samples was determined by Archimedes method. The Vickers microhardness of the bulk samples was measured using a microhardness tester by applying a load of 300 g for 10 s on the polished surfaces of the samples. For each sample, 10 separate indents were created on the investigated surface.

The Solartron 1285 potentiostat was applied for corrosion measurements. The corrosion resistance of different samples was measured in Ringer's solution (simulated body fluid with composition: NaCl: 9g/l, KCl: 0.42 g/l, $CaCl_2$: 0.48 g/l, $NaHCO_3$: 0.2 g/l) applying potentiodynamic mode with scan rate 0.5 mV/s at temperature of 37 ± 1°C, controlled by thermostat. The corrosion test was run in EG&G K0047 corrosion cell. The counter electrode consisted of two graphite rods, and a platinum electrode was used as the reference electrode. The surface area exposed to the electrolyte was 0.5 cm^2. Polarization curves were obtained for each specimen in the potential range for –2 to 3 V. The corrosion potentials (E_{corr}) and corrosion current densities (I_{corr}) were estimated from the Tafel extrapolations of the corrosion curves, using CorrView software.

3. Results and discussion

The aim of this research was synthesis of β type Ti-x at. % Mo (x = 15 and 23) alloys by mechanical alloying and powder metallurgy methods. The structure changes during MA was investigated. Fig. 1 shows typical XRD patterns from the me-

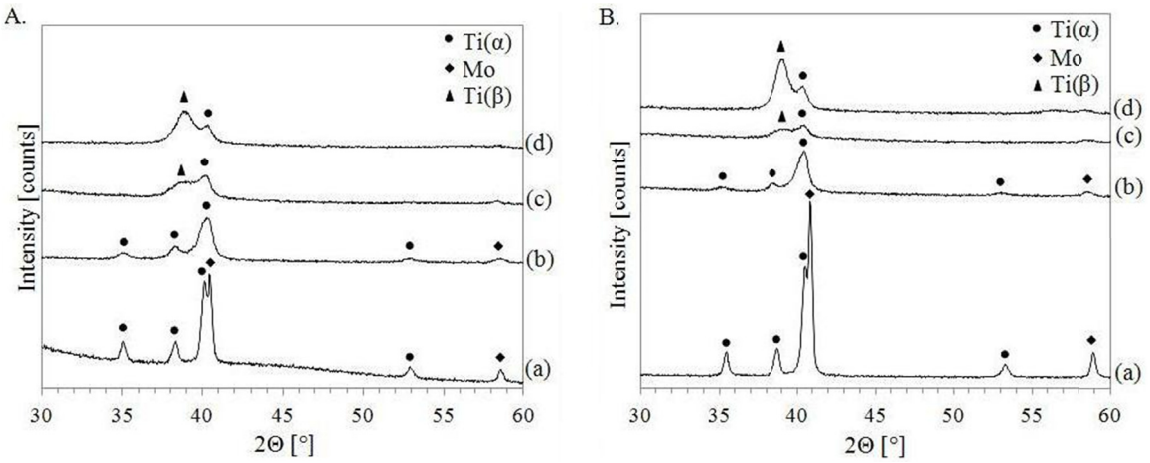

Fig. 1. XRD spectra of Ti-15 at.% Mo (A) and Ti-23 at. % Mo (B) mechanically alloyed for different times: 15 min (a), 5 h (b), 15 h (c) and 48 h (d)

chanically alloyed Ti-15 at. % Mo and Ti-23Mo at. % materials after different milling times. For example, Fig. 1a shows the XRD pattern of the microcrystalline titanium and molybdenum powders after 15 min of MA Ti-15 at. % Mo. After 5 h of MA the (110) plane from cubic Mo crystal structure disappeared, and additionally after 15 h new phase Ti(β) (2 theta = 38.892 deg) is forming. The high plastic deformations of the powders results in high density of dislocation lines and subsequently subgrains formation, which may finally leads to amorphisation [14]. After 48 h of mechanical alloying the powders are almost amorphous (Fig.1c) and the crystallite sizes calculated by the application of Williamson-Hall approach were 7.2 and 13 nm for 15 and 23 at. % of Mo content in Ti-Mo alloy, respectively (Fig. 2). The MA process allows to transform Ti(α) to Ti(β) due to the molybdenum content and milling time (15 h). Finally, it is necessary to mention that application of MA process reduces not only the microstructure of so produced alloys but also generated the phase transition Ti(α) $\rightarrow$ Ti(β).

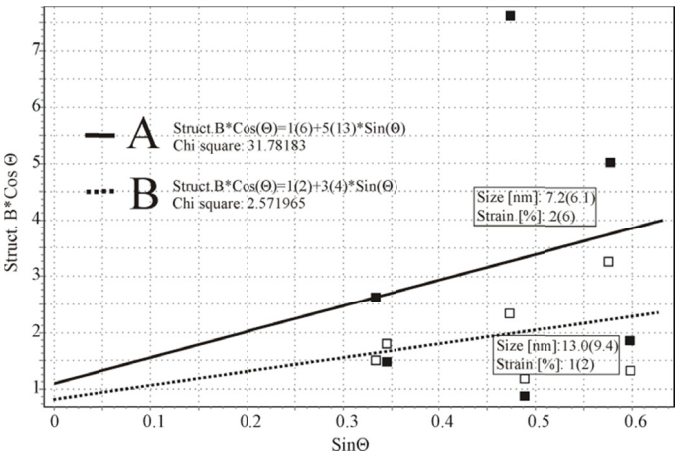

Fig. 2. Linear Williamson-Hall plots with obtained equation and estimated structure size and strain factors based on the XRD spectra of Ti-15 at.% Mo (a) and Ti-23 at. % Mo (b) powder materials after 48h of mechanical alloying

The low temperature sintering at 750, 800 or 850°C for 30 min results in crystallization and bulk materials formation (Fig. 3). Additionally to the main Ti(β) phase, the second Ti(α) phase is detected. Except the value of the heat treatment temperature, the amount of molybdenum in the Ti-Mo alloy is sensitive of the final phases content of so produced alloys.

The smooth and porous Ti-x at. % Mo alloys surfaces are presented in Fig. 4. The relative density of the bulk alloys were measured to be 85 and 90% for 15 at. % and 23 at. %, respectively. The results of EDS analysis of the surfaces of sintered Ti-Mo materials are shown in Fig. 4, too. It can be confirmed that synthesized alloy mainly consists of Ti 15 at. % Mo and 23 at. % Mo with small content of α-Fe. The presence of iron atoms in the synthesized alloys could be explained by Fe impurities trapped in the MA powders from erosion of the milling media. The change of the porosity in Ti-Mo system leads to a distribution of the properties. A porous structure can significantly reduce the Young's modulus of studied alloys. The elastic modulus of porous biomaterials can by easily fitted to the elastic modulus of bones by control of porosity. As a result the shielding effect of implant and degradation of bone can by reduced or eliminated. The open and interconnected porosity enables ingrowth of bone tissues into implant surface, formation of blood vessels and natural fixation of the implant in the human skeleton [5-7,15]. Several factors have been demonstrated to have an influence on bone ingrowth into porous implants, such as the porous structure (pore size, pore shape, porosity and interconnecting pore size) of the implant, duration of implantation, biocompatibility, implant stiffness, micromotion between the implant and adjacent bone, etc. [16].

The Vickers microhardness of the sintered alloys exhibit various distribution corresponding to constitutional change of

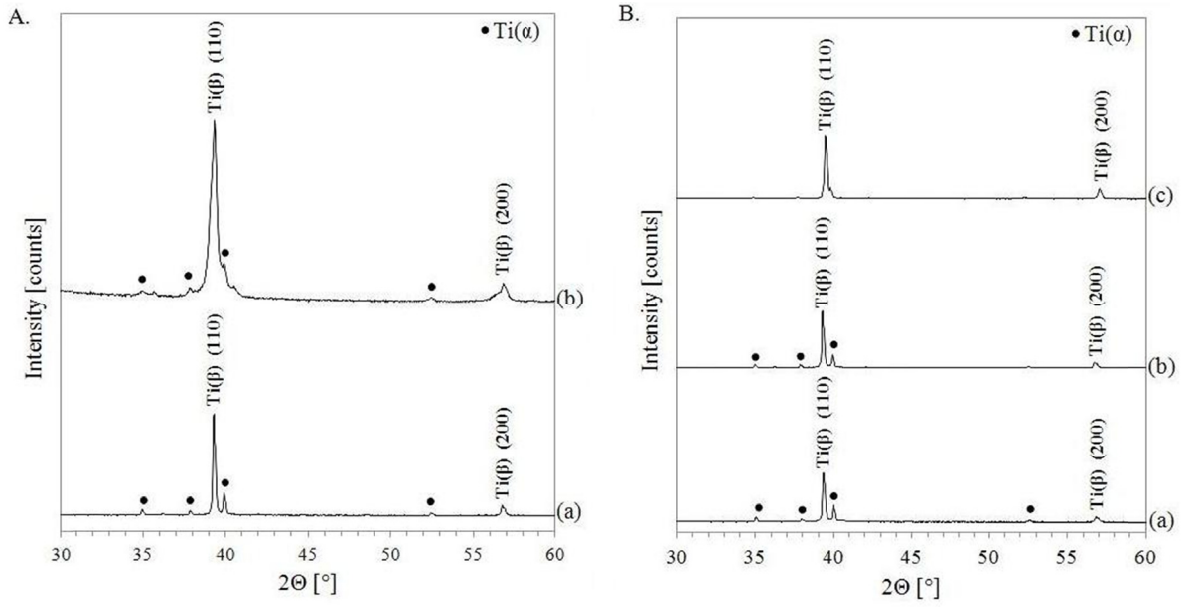

Fig. 3. A. XRD spectra of Ti-x at.% Mo mechanically alloyed for 48 h and annealed for 800ºC/0.5 h: x = 15 at. % and x = 23 at. % (b). B. XRD spectra of Ti-15 at.% Mo mechanically alloyed for 48 h and annealed for 750 (a), 800 (b) and 850ºC (c) for 0.5 h

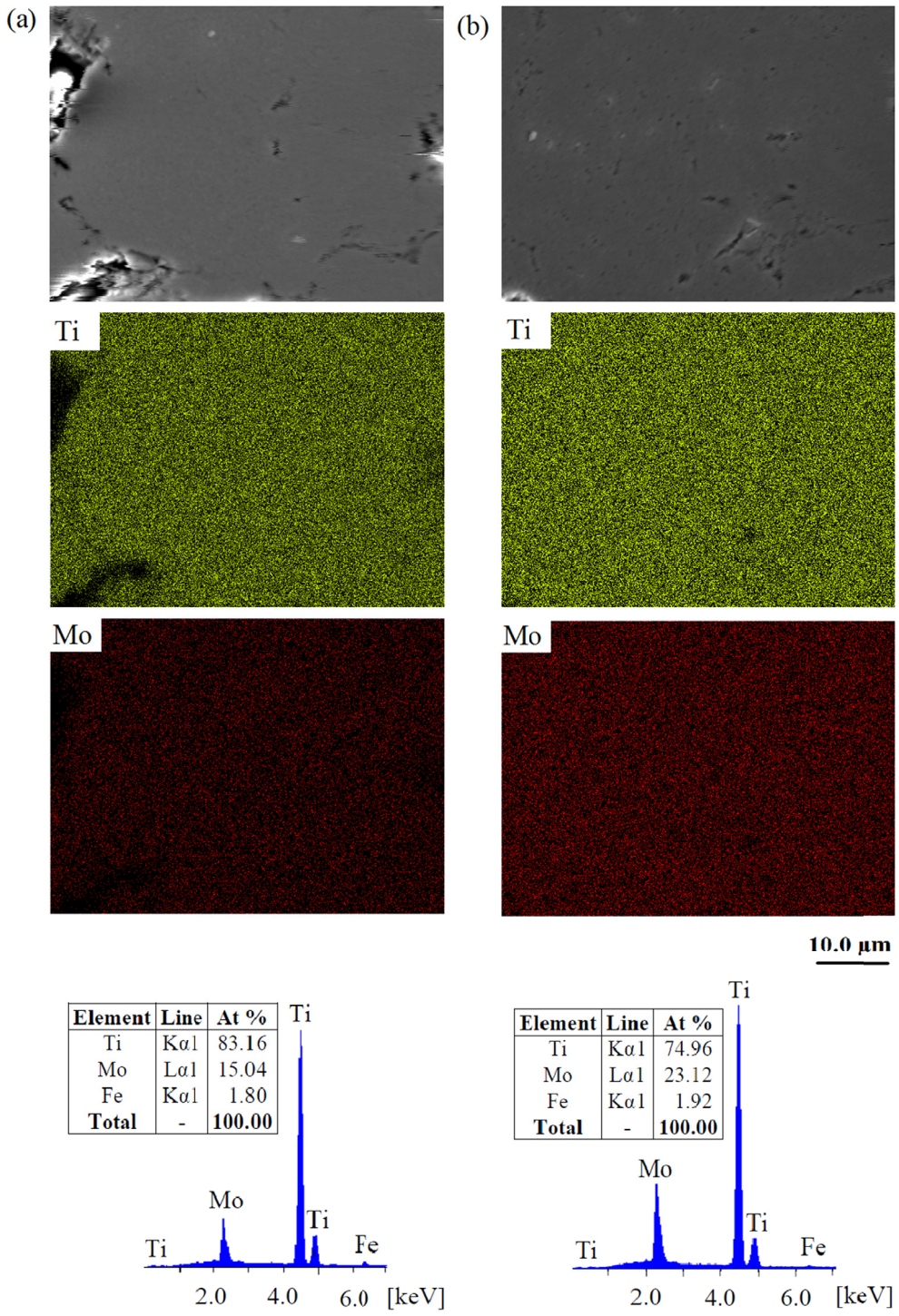

Fig. 4. SEM micrographs, EDS mapping of the Ti and Mo distribution and EDS spectra of Ti-15 at.% Mo (a) and Ti-23 at.% Mo (b) alloys mechanically alloyed for 48 h and annealed at 800°C for 0.5 h

microstructure and increase with the rise of Mo contents. The Vickers hardness of Ti23Mo alloy (350 HV0.3) is higher than that of Ti15Mo alloy (244 HV0.3). This effect is directly connected with chemical modification as well as the microstructure refinement during the MA process and next also obtained in the final sinters homogenized phase composition.

The corrosion resistance of the Ti15Mo and Ti23Mo alloys in Ringer solution was investigated (Table 1, Fig. 5). Using CorrView software, from the Tafel extrapolations of the

TABLE 1

Theoretical density (ρ_{th}), porosity (P), microhardness (HV0.3), corrosion current density (I_{cor}) and corrosion potential (E_{cor}) of bulk Ti – x at.% Mo alloys

x	ρ_{th} [g/cm^3]	P [%]	HV0.3	I_{cor} [µA/cm^2]	E_{cor} [V]
15	5.37	10	244	98.05	–1.37
23	6.70	9	350	70.93	–0.79

recorded potentiodynamic corrosion curves, corrosion current density (I_{cor}) and corrosion potential (E_{cor}) was determined. The addition of Mo to Ti-Mo alloy has also a positive effect on the corrosion resistance in Ringer's solution. Ti23Mo alloy has better corrosion resistance (I_{cor} = 70.93 μA/cm^2, E_{cor} = –0.79 V) than Ti15Mo alloy (I_{cor} = 98.05 μA/cm^2). Till now, the best corrosion resistance shows Ti-23 at.% Mo-3 wt. % 45S5 Bioglass composite after electrochemical etching and Ca-P deposition (I_{cor} = 0.0168 μA/cm^2, E_{cor} = –0.44 V) [17]. Additionally, the corrosion potential (E_{cor}) is shifted to the more nobler direction (E_{cor} = –0.44 V).

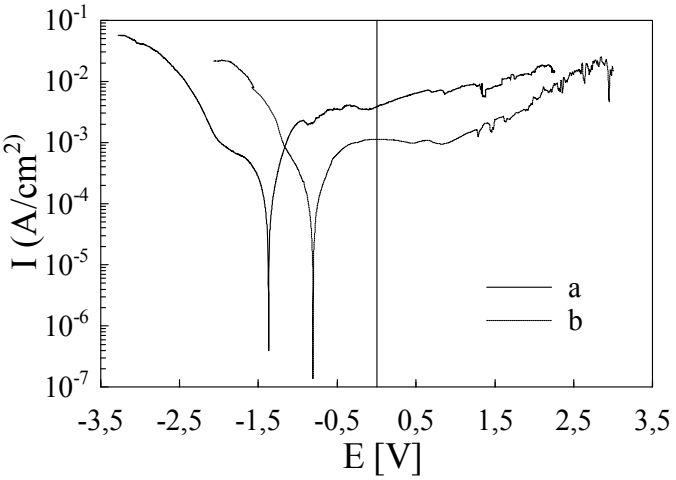

Fig. 5. Potentiodynamic polarization curves of the bulk Ti-15 at.% Mo (a) and Ti-23 at. % Mo (b) alloys in the Ringer solution at 37°C

Published results clearly demonstrate that powder manufacturing routes produce Ti-based implants that are suitable for biomedical applications [15,18]. More research is needed into the biocompatibility and functionality of synthesized Ti-Mo alloys. Many different methods for producing nanocrystaline and/or fine grained structures are available [7]. They are mainly based on the production of fine grained powders (down the nanometer scale) and a subsequent powder metallurgy for consolidation [4]. It is well proven that the a mechanical properties of Ti-based alloys can be significantly enhanced by refinement of grain structure. Grain refinement is a key principle in the strengthening of engineering alloys. Our results show that the crystal structure of solution treated alloys are sensitive to Mo contents. When Mo content increases the β phase becomes the only dominant phase.

Nanocrystalline and ultrafine grained metals due to extremely small grain sizes enhance physicochemical, mechanical and biological properties compared with the corresponding materials with microcrystalline grain size [18,19]. Valiev and co-workers apply a process known as equal channel angular pressing (ECAP), which is a viable processing route to grain refinement and property improvement [7,19]. Cytocompatibility tests utilizing fibroblast mice cells L929 were carried out. After nanostructuring, fibroblast colonization of the cp Grade 4 titanium surface increases.

A small degree of residual porosity after powder compaction has also played a role in the cell adhesion. It was proposed that an increased area of the surface defects exposed to the cell culture and to a larger degree of surface electron delocalization caused enhanced cell adhesion.

4. Conclusions

The aim of this research was synthesis of titanium-molybdenum (Ti-x at. % Mo, x = 15 and 23) alloys. The influence of Mo content and heat treatment temperature on phase transitions (Ti(α)-Ti(β)) were studied. The following conclusions can be withdrawn:

- longer MA time increase the content of Ti(β)-phase in Ti-x at. % Mo system,
- crystallization of the obtained material upon annealing lead to the formation of a Ti(β) type alloys,
- with the increase of Mo contents in Ti-x at. % Mo system increase of β-phase is noticeable for obtained sinters,
- with the increase of annealing temperature more Ti(β)-phase in Ti-x at. % Mo system is noticeable,
- with the increase of Mo contents in Ti-x at. % Mo system an increase of microhardness in alloys is observed,
- the addition of Mo to Ti-Mo alloy has a positive effect on the corrosion resistance in Ringer's solution.

Acknowledgements

The work has been financed by Polish Ministry of Science and Higher Education within statutory activity.

REFERENCES

[1] H.J. Rack, J.J. Qazi, Mater. Sci. Eng. C**26**, 1269 (2006).
[2] M. Geetha, A.K. Singh, R. Asokamani, A.K. Gogia, Progr. Mat. Sci. **54**, 397 (2009).
[3] Y. Estrin, C. Kasper, S. Diederichs, R. Lapovok, J. Biomed. Mater. Res. A **90**, 1239 (2009).
[4] C. Suryanarayna, Prog. Mater. Sci. **46**, 1 (2001).
[5] T.J. Webster, J.U. Ejiofor, Biomaterials **25**, 4731 (2004).
[6] M. Kaczmarek, M.U. Jurczyk, B. Rubis, A. Banaszak, A. Kolecka, A. Paszel, K. Jurczyk, M. Murias, J. Sikora, M. Jurczyk, J. Biomed. Mater. Res. **102**A, 1316 (2014).
[7] R.Z. Valiev, I.P. Semenova, V.V. Latysh, H. Rack, T.C. Lowe, J. Petruzelka, L. Dluhos, D. Hrusak, J. Sochova, Adv. Eng. Mater. **10**, 1 (2008).
[8] R. Bawa, G.F. Audette, I. Rubinstein (Ed.), Handbook of Clinical Nanomedicine: Nanoparticles, Imaging, Therapy, and Clinical Applications, Pan Stanford Publishing Pte. Ltd., ISBN 978-981-4669-20-7 (2015).
[9] D. Kuroda, M. Niinomi, M. Morinaga, Y. Kato, T. Yashiro, Mater. Sci. Eng. A **243**, 244 (1998).

[10] A.T. Sidambe, Materials **7**, 8168 (2014).
[11] E. Kobayashi, H. Doi, M. Takahashi, T. Nakano, T. Yoneyama, H. Hamanaka, J. Jpn. Soc. Dent. Mater. Dev. **14**, 406 (1995).
[12] E. Kobayashi, H. Doi, T. Yoneyama, H. Hamanaka, S. Matsumoto, K. Kudaka, J. Jpn. Soc. Dent. Mater. Dev. **14**, 321 (1995).
[13] M. Niinomi, Sci. Techn. Adv. Mater. **4**, 445 (2003).
[14] J.J. Benjamin, Sci. Am. **234**, 40 (1976).
[15] P.I. Brånemark, The Journal of Prosthetic Dentistry **50**, 399 (1983).
[16**]** B.C. Ward, T.J. Webster, Mater. Sci. Eng. C **27**, 575 (2007).
[17] K. Jurczyk, A. Miklaszewski, M.U. Jurczyk, M. Jurczyk, Materials **8**, 8032 (2015).
[18] L. Mishnaevsky Jr, R. Levashov, R.Z. Valiev, J. Segurado, I. Sabirov, N. Enikeev, S. Prokoshkin, A.V. Solov'yov, A. Korotitskiy, E. Gutmanas, I. Gotman, E. Rabkin, S. Psakh'e, L. Dluhoš, M. Seefeldt, A. Smolin, Mater.Sci. Eng. R: Reports **81**, 1 (2014).
[19] R.Z. Valiev, M.J. Zehetbauer, Y. Estrin, H.W. Höppel, Y. Ivanisenko, H. Hahn, G. Wilde, H.J. Roven, X. Sauvage, T.G. Langdon, Adv. Eng. Mater. **9**, 527 (2007).